ICES Journal of Marine Science, 2023, **0**, 1–18
DOI: 10.1093/icesjms/fsad113
Original Article

ICES International Council for the Exploration of the Sea
CIEM Conseil International pour l'Exploration de la Mer

Temperature-dependent spawning behaviour and larval thermohaline associations of Bering Sea groundfish

L. Vary [1,*,†], L. Rogers [2], M. Harte[3], R. Howard[3], and L. Ciannelli[3]

[1]Marine Resource Management, Oregon State University, Corvallis, OR 97331, USA
[2]Alaska Fisheries Science Center, National Oceanic and Atmospheric Administration, Seattle, WA 98115, USA
[3]College of Earth, Ocean, and Atmospheric Sciences, Oregon State University, Corvallis, OR 97331, USA

[*] *Corresponding author:tel: 1-207-252-8601;* e-mail: Vary.laura@gmail.com.
[†]Present address: Puget Sound Partnership, Olympia, WA 98501, USA.

The Bering Sea is a productive large marine ecosystem that supports numerous commercial fisheries, while climate change is introducing rapid warming and freshening, especially in coastal water. The success of early life stages of marine fish can impact adult abundance levels; little is known about how behavioural or physiological plasticity in relation to environmental changes at one stage (e.g. spawning) may affect survival during subsequent stages (e.g. larvae), nor whether trade-offs exist that affect how a species demonstrates such plasticity. We utilized a statistical approach to examine phenological and geographical flexibility in spawning behaviour for four species of groundfish. *In situ* sea surface temperature (SST) and salinity (SSS) associations were also estimated by statistical models for six species of groundfish larvae. All species exhibited greater spawning geography flexibility than phenological flexibility during the egg stage. All larval stages exhibited specific temperature and salinity associations across unique combinations of SST and SSS. These species-specific patterns, in the context of potential climate change impacts, suggest that flexibility in spawning behaviour may not adequately compensate for the presence of unfavourable habitats at the larval stage.

Keywords: climate change, early life stages, generalized additive models, phenology.

Introduction

Consistent spawning behaviour in fish likely increases the success of vulnerable early life stages (eggs and larvae) by increasing the probability of matching larval development with peaks in prey abundance and/or favourable oceanographic and habitat conditions during ontogeny (Durant *et al.*, 2007; Bacheler *et al.*, 2009; Siddon *et al.*, 2011; Ciannelli *et al.*, 2015; McQueen and Marshall, 2017; Asch *et al.*, 2019; Biggs *et al.*, 2021). However, climate change creates disjointed dynamics between spawning behaviour and the ideal conditions for larvae, with far-reaching consequences for adult populations and the economies that rely on thriving fisheries (Poloczanska *et al.*, 2013; Asch *et al.*, 2019). Even in the presence of spawning geographic or phenological flexibility (i.e. behavioural or physiological plasticity), the survival of later stages may be reduced if exposed to novel and unfavourable oceanographic and habitat conditions (Cushing, 1990; Durant *et al.*, 2007; Bacheler *et al.*, 2009; Ciannelli *et al.*, 2015; Logerwell *et al.*, 2020). Whether there is a tradeoff between spawning phenology and geographic flexibility remains unclear.

Marine fish at large have either demonstrated interannual flexibility in the environmental conditions at which they spawn (geographic spawners, constrained by place) or the location at which they spawn (environmental spawners, constrained by environmental processes) (Ciannelli *et al.*, 2007; Bacheler *et al.*, 2012; Asch, 2015; Porter and Ciannelli, 2018; Asch *et al.*, 2019). The type and degree of plasticity a species may exhibit may depend upon factors like species-specific life history characteristics and habitat usage. While past research has identified trait complexes likely to correlate with more plasticity in spawning phenology (e.g. Ciannelli *et al.*, 2007; Bacheler *et al.*, 2012; Asch, 2015), patterns in spatial shifts are typically not explicitly investigated nor investigated in conjunction with phenology. Thus, it is plausible that spawning plasticity may exist in more species than currently identified, but quantification of such plasticity in space and time and how this may relate to ecological characteristics has yet to be established for most species.

Groundfish in the Bering Sea (BS) are adapted to the variable environmental characteristics of the region and exhibit spawning strategies that increase the probability of survival for their young (Siddon *et al.*, 2011, 2019; Asch *et al.*, 2019; Logerwell *et al.*, 2020). Despite known evolutionary constraints on spawning location and spawning timing, past studies note that plasticity in behaviour and physiology can lead to variable spawning behaviour (Kjesbu and Witthames, 2007). In the BS, the historic interannual variability provides an opportunity to evaluate the relationship between the environment and the phenology and geography of spawning in groundfish (Logerwell *et al.*, 2020). Additionally, the impact that spawning plasticity, if present, may have on larvae can be further understood by studying the thermohaline associations of larvae in the BS. We thus sought to quantify the degree to which BS groundfish exhibit spawning flexibility and whether changes in spawning timing and/or locations are likely to expose larval stages to unfavourable habitat conditions.

Upon hatching, larvae in the BS tend to concentrate into specific water masses, defined by salinity and temperature, and are transported with prevailing currents; such associations are typically consistent interannually and are extremely important

Received: 17 December 2022; **Revised:** 19 June 2023; **Accepted:** 19 June 2023

for larval development and dispersal processes (Doyle *et al.*, 2009; Siddon *et al.*, 2011; Ciannelli *et al.*, 2015; Swearer *et al.*, 2019; Logerwell *et al.*, 2020). While larval growth and development are closely temperature-dependent, salinity also exerts strong, and currently understudied, impacts on larval development and transport. Previous studies indicate that ranges outside a species' salinity window can lead to osmoregulatory stress and abnormal development; salinity variance also impacts early life stage buoyancy, thereby impacting transport (Holliday and Blaxter, 1960; Bœuf and Payan, 2001; Munk, 2016; Spencer *et al.*, 2020). However, there is a paucity of information on habitat suitability for BS larvae as a function of both temperature and salinity (Doyle *et al.*, 2009; Logerwell *et al.*, 2020). While hydrographic domains on the BS continental shelf exhibit specific ranges of temperature and salinity, these ranges may be altered in the future, especially in coastal areas, as temperatures and freshwater runoff increase. As coastal regions freshen, it is critical to take a multi-dimensional approach to habitat suitability of early life stages and investigate salinity associations alongside thermal preferences (Dávila *et al.*, 2002; Sejr *et al.*, 2017; Boone *et al.*, 2018; Ciannelli *et al.*, 2022b).

Examining connections of larval environmental associations to their species' spawning behaviour offers a nuanced perspective of ecosystem dynamics and drivers of early life stage success. Hence, the goals of this study were as follows:

(1) Evaluate larval biogeography in association with *in situ* measurements of sea surface temperature (SST) and sea surface salinity (SSS) for six species of groundfish larvae.
(2) Evaluate the degree to which groundfish modify their spawning behaviour in space or time across a subset of groundfish.

As the BS ecosystem rapidly garners new ecosystem-wide dynamics through climatic forcing and anthropogenic climate change, it is increasingly important to look towards early life stages that can reveal species vulnerabilities and large-scale patterns of change. While this study is focused on the BS, it is relevant to other sub-arctic regions and coastal nursery areas, which are also experiencing warming and increased spring and summer discharge of freshwater (Dávila *et al.*, 2002; Gibson *et al.*, 2002; Royer and Grosch, 2006; Sejr *et al.*, 2017; IPCC: Summary for Policymakers, 2022).

Methods

Study region

The BS shelf is divided into three domains, delineated by bathymetry: the coastal domain (depths < 50 m), the middle domain (depths between 50 and 100 m), and the outer domain (depths between 100 and 200 m; Figure 1). Distinctive levels of temperature, salinity, and other characteristics of vertical structure comprise three hydrographic boundaries persistent on the broad BS continental shelf through much of the year, further delineating these domains (Kinder and Schumacher, 1981). In May, isotherms in the coastal domain roughly mirror the coastline, and temperatures range from 0 to 3°C. In the summer, temperatures range from 5 to 11°C, with warmer temperatures in shallower waters on average. In September, temperatures range from ~8 to 10°C. The lowest salinities (~30 ppt) occur in the coastal domain in the summer due to freshwater input (Luchin *et al.*, 1999). In this coastal

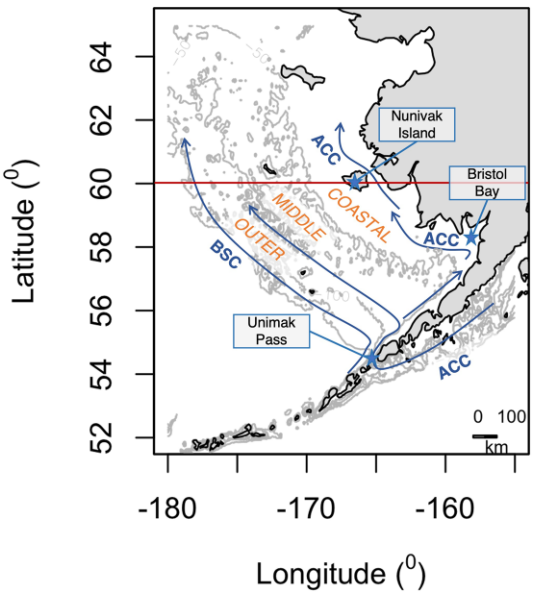

Figure 1. Hydrographic domains of the Bering Sea (BS) region: the coastal domain (<50 m), the middle domain (>50 m and <100 m), and the outer domain (>100 m and ≤200 m). The red line at 60°N delineates the southern BS from the northern BS. Modified from Kinder and Schumacher (1981).

domain, temperature and salinity are generally homogenous with depth (Kinder and Schumacher, 1981).

Each domain has unique hydrographic features and seasonality, as described above. Additionally, the BS cold pool is a feature of persistent, cold, and dense water that rests on the ocean floor of the BS shelf primarily during late spring and summer months. It occurs in the middle domain, and its spatial spread is closely associated with sea ice formation, melting, and buoyancy-driven mixing (Kinder and Schumacher, 1981; Wyllie-Echeverria and Wooster, 1998; Duffy-Anderson *et al.*, 2006). As sea ice forms in the fall, brine water is ejected, creating a layer of cold, dense water that sinks to the shelf floor (Kinder and Schumacher, 1981). The cold pool affects adult species assemblages at depth; it creates a thermal barrier within the water column as well as latitudinally, separating species between Arctic and sub-Arctic bioregions and establishing different physical habitats for species present in the benthos compared to the upper water column (Wyllie-Echeverria and Wooster, 1998). In this way, the cold pool can exert control on adult populations and spawning migrations as species move throughout the BS.

At the surface of the middle domain, temperatures in the spring and summer range from 2 to 8°C and are spatially heterogenous across the domain; the highest temperatures occur in August (Luchin *et al.*, 1999). In September, temperatures range between 7 and 8°C. Surface salinities are typically ~32 ppt across the spring and summer (Luchin *et al.*, 1999). The outer domain has the greatest degree of stratification of the three domains (Kinder and Schumacher, 1981). Spring and summer surface temperatures vary from 2 to 9°C on average; highest salinities in the BS occur in this domain during the late spring (Luchin *et al.*, 1999). Surface currents and bathymetric features also influence the physical dynamics of the BS. The Alaska Coastal Current enriches the southeastern BS with warmer, fresher, and nutrient-rich waters, while the Bering Slope Current (BSC) generates hydrographic insta-

bilities promoting the formation of nutrient-concentrating eddies along the shelf edge (Mizobata and Saitoh, 2004; Mizobata *et al.*, 2006; Sambrotto *et al.*, 2008; Stabeno *et al.*, 2016). The Bering, Pribilof, and Zhemchug canyons, present along the shelf edge, interact with surface currents, including on-shelf flow and the BSC (Duffy-Anderson *et al.*, 2006; Vestfals *et al.*, 2014; Stabeno *et al.*, 2016).

Study species

This study focused on five Pleuronectids, Alaska plaice (*Pleuronectes quadrituberculatus*), flathead sole (*Hippoglossoides elassodon*), northern rock sole (*Lepidopsetta polyxystra*), rex sole (*Glyptocephalus zachirus*), and yellowfin sole (*Limanda aspera*), as well as two Gadid species: Walleye pollock (*Gadus chalcogrammus*) and Pacific cod (*Gadus macrocephalus*). These species span diverse life histories, habitat preferences, spawning timing and locations, and ecological niches; they are additionally ecologically and commercially important to the BS region (Table 1). Fisheries with the most economic value and harvest volumes are walleye pollock, Pacific cod, and yellowfin sole (National Marine Fisheries Service and National Oceanic and Atmospheric Administration, 2021; NOAA Fisheries, 2022). Alaska plaice, flathead sole, rex sole, and walleye pollock were the only species included in the egg analyses due to their consistent presence in egg survey records throughout the southeastern BS. Due to the species' lack of presence in larval records, rex sole was not included in the larval analyses.

Ichthyoplankton and environmental data

The data used for this study were collected by the Ecosystems and Fisheries-Oceanography Coordinated Investigations (EcoFOCI) programme of NOAA's Alaska Fisheries Science Center (AFSC). This multidecadal, spatially expansive ichthyoplankton time series and the characteristics of the BS region (e.g. interannual environmental variability and the rapid onset of climate change) are unique and provided a strong foundation to evaluate our research questions regarding environmental associations and plasticity (Sheffield Guy *et al.*, 2014; McClatchie *et al.*, 2016). Sampling occurred from February to October, with the most frequent sampling in May–September; sampling design systematically covered the southeastern BS region to depths up to 4060 m (Table 2). Ichthyoplankton hauls were conducted with bongo nets of two mesh sizes (333 or 505 μm); however, these mesh size differences have proved to have little impact on ichthyoplankton catch rates in this region (Shima and Bailey, 1994; Boeing and Duffy-Anderson, 2008). The spatial extent of the surveying effort is provided in Supplementary Information Section 1.

Environmental data include Conductivity Temperature Depth (CTD) profiles that were collected concurrently with egg and larval sampling; these data were used to determine larval environmental associations. Surface salinity (SSS) and temperature (SST) values were averaged across the upper 10 m of the water column to represent the upper-surface mixed layer. This depth limit was utilized because many groundfish larvae in the Bering Sea are typically found in the mixed layer (Olivar and Sabatés, 1997; Smart *et al.*, 2013).

We interpolated average CTD data of the surface 10 m over the southeastern BS for the month of May–September, from 1997 to 2016, to better understand how temperature and salinity tend to vary across the region in warm and cold phases (Supplementary Information Section 2). These two months were isolated because the majority of observations for all species except for yellowfin sole occurred during the month of May, while the majority of yellowfin sole observations occurred in September. However, ichthyoplankton observations used in this study's analyses were not constrained to these two months. These SST and SSS maps represent two combined warm regimes (2001–2005 and 2014–2016) and one cold regime (2006–2013) for these two months (Stabeno *et al.*, 2017; Baker, 2021). All maps were interpolated using a local quadratic (second degree) regression fitting function with a span of 0.15 (*loess* function from the R package *stats,* version 3.6.2; R Core Team, 2021); values >30 km from observations were removed from the interpolated figures. Surface temperature-salinity plots were also evaluated within each domain (coastal, middle, and outer) across warm and cold regime years by plotting raw (i.e. not interpolated) SST against SSS, isolated by domain, and colour-coding points according to the regime (Figure 2).

Ichthyoplankton data were temporally trimmed to focus the extent to known spawning times and periods in which larvae are present in the water column (Table 3). Data were clipped to remove stations >30 km from a positive observation for each species. This operation ensures that we focus the analyses on the areas consistently inhabited by the target species. All explorative and processing techniques were conducted in RStudio version 4.1.0 (R Core Team, 2021).

Spawning behaviour analyses were conducted with egg ichthyoplankton data, which were matched to an average regional temperature index, calculated across one month over a consistent sub-area of the study region, for each year of the study (henceforth referred to as the "regional temperature index"). We assumed that egg data are adequate proxies for spawning location, an assumption aligned with numerous other studies (e.g. Bellier *et al.*, 2007; Ciannelli *et al.*, 2007; Bacheler *et al.*, 2009, 2012; Lelièvre *et al.*, 2014). For each species, the peak in egg catch per unit effort (CPUE) by month across years was identified, and the associated regional temperature index was then calculated for the period two months prior to the egg CPUE peak. For all egg species (Alaska plaice, flathead sole, walleye pollock, and rex sole), the peak in egg catch occurred in May; thus, the regional temperature index was created based on March values. This lag was adopted to account for multiple dynamics of reproduction: the length of time during which groundfish species migrate into the spawning habitat, the length of time during which groundfish are undergoing gonadal maturation, and the temporal lag between when spawning adults are present at the spawning location and when eggs are collected (Lowerre-Barbieri *et al.*, 2011). The regional temperature index is calculated as the average sea surface temperature (SST) values in a 1° × 1° grid across the southeastern BS region with following latitudinal and longitudinal ranges: 55.5°N–57.5°N and 168.5°W–163.5°W. The temperature data used to calculate regional temperature indices were obtained from the NOAA COBE SST dataset ("COBE SST: NOAA Physical Sciences Laboratory, 2005").

Additional cruise information, including name, dates of vessel deployment, and number of stations sampled, can be found in the Supplementary Information Section 2.

Table 1. Description of ecological and early life history characteristics for each study species.

	Gadus chalcogrammus	*Gadus macrocephalus*	*Glyptocephalus zachirus*	*Hippoglossoides elassodon*	*Lepidopsetta polyxystra*	*Limanda aspera*	*Pleuronectes quadrituberculatus*
Common name	Walleye pollock	Pacific cod	Rex sole	Flathead sole	Northern rock sole	Yellowfin sole	Alaska plaice
Reproductive season	February to May[1]	March and April[1]	October to May[1]	February to July[1]	December to March[11]	March to August[13]	April to May[14]
Reproductive habitat	Upper slope and outer shelf [1]	Middle to outer shelf[6]	Deep water, outer shelf[8]	Middle shelf[10]	Middle and outer shelf[11]	Coastal shelf[1,2]	Middle shelf[14]
Adult habitat	Mid-water pelagic[1]	Deep-water benthic[1]	Demersal, sand/mud substrate[1]	Demersal, shelf and cont. slope[1]	Demersal, muddy substrate[12]	Demersal, sandy substrate[9]	Demersal, shallows; sand/mud substrate[14,15]
Egg classification	Pelagic[1]	Demersal, adhered[7]	Pelagic[1]	Pelagic[1]	Demersal, adhered[11]	Pelagic[2]	Pelagic[2]
Larval length at transformation (mm SL)	25–40[2]	25–35[2]	>50[2]	18–21[2]	15–18.6[2]	15–17[2]	>10.7[2]
Age at maturity	3–4 years[2]	2–3 years[1]	3–4 years (M), 5–9 years (F)[1]	2–3 years[1]	7 years[10]	4–7 years[2]	7 years[18]
Lifespan	12 years[3]	13 years[1]	24 years[1]	21 years[1]	17–19 years[2]	17–19 years[2]	Over 30 years[18]
Commercial fishing pressure (biomass estimate)/acceptable biological catch; metric tons)	2 961 540/1 677 241[4,5]	305 678/144 405[4,5]	38 598/17 189[4,5,9,†]	148 077/62 567[4,5]	314 380/140 306[4,5,†]	867 221/313 477[4,5]	204 132/31 657[4,5]

[†] Acceptable biological catch for rex sole is the total for the "other flatfish" NPFMC management unit; Acceptable biological catch for northern rock sole is for the "rock sole" NPFMC management unit.
[1] (Matarese *et al.*, 2003);
[2] (NOAA AFSC, 2021);
[3] (NOAA Fisheries, 2021);
[4] (National Marine Fisheries Service and National Oceanic and Atmospheric Administration, 2021);
[5] (NOAA Fisheries, 2022);
[6] (Neidetcher *et al.*, 2014);
[7] (Laurel and Rogers, 2020);
[8] (Abookire and Bailey, 2007);
[9] (Wilderbuer, 2015);
[10] (Porter and Ciannelli, 2018);
[11] (Wilderbuer *et al.*, 2016);
[12] (Lanksbury *et al.*, 2007);
[13] (TenBrink, 2022).
[14] (Duffy-Anderson *et al.*, 2010);
[15] (Bailey *et al.*, 2003);
[16] (Zhang *et al.*, 1998).

Table 2. Description of spatial, temporal, and technical attributes of data used in this study.

Data source	Variables provided	Relevant species	Life stage	Instrument	Geographic range	Depth range (m)	Seasonality/Year coverage	Additional citations
AFSC EcoFOCI ichthyoplankton cruises	Catch per 10m^2 (μ), latitude (ϕ), longitude (λ), bottom depth (b), year (yr), day of year (d)	AP, FHS, NRS, PC, WP, RS, and YFS	Egg and larval	60 cm bongo net; mesh size of either 333 or 505μm	51.67–66.5°N, 157.81–179.98°W	0–4 060	February–October 1979, 1988, 1991–2016	Ciannelli *et al.*, 2007; Bacheler *et al.*, 2012; Porter and Ciannelli, 2018
AFSC EcoFOCI CTD deployments	*In situ* sea surface temperature (*SST*), *in situ* sea surface salinity (*SSS*)	AP, FHS, NRS, PC, WP, and YFS	Larval	19 + version 2 SeaCAT Profiler, Sea-Bird Scientific 49 FastCAT sensor	51.88–73.56°N, 149.41–178.17°W	0–2 102	February–October 1997–2016	Eisner et al., 2018; Porter and Ciannelli, 2018
NOAA COBE SST dataset, Japanese Oceanographic Data Center	Regional sea surface temperature (*reg.SST*)	AP, FHS, WP, and RS	Egg	Satellite	55.5–57.5°N, 163.5 –168.5°W	Surface	March 1979–2016	Folland and Parker, 1995; Ishii et al., 2005; Japan Meteorological Society, (n.d.)

Attributes reflect data prior to trimming and modification for analytical purposes.

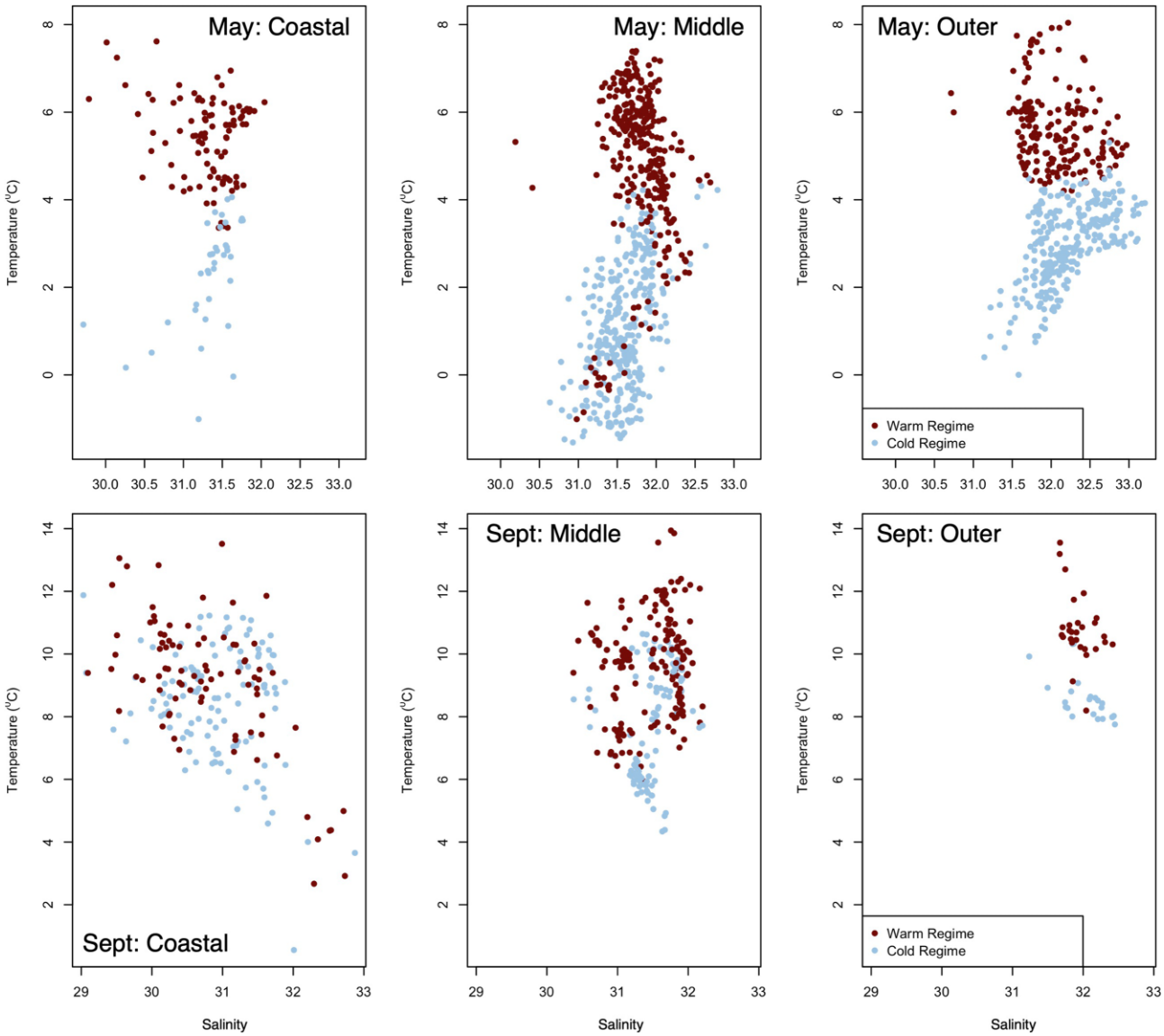

Figure 2. Comparison of SST and SSS across hydrographic domains for warm regime years (2001 through 2005 and 2014 through 2016) and cold regime years (2006 through 2013) in both May (top panel) and September (bottom panel).

Analytical framework

Our analytical goals were twofold: first, we sought to quantify larval associations with two environmental parameters, sea surface temperature (SST) and sea surface salinity (SSS); second, we sought to quantify the spatial and temporal dynamics of spawning behaviour in relation to temperature. To measure these relationships, we developed generalized additive models (GAMs) of varying formulations. GAMs are built with nonlinear smoothing terms, allowing dependent and independent covariate relationships to be modelled in a biologically realistic manner (Hastie and Tibshirani, 1986; Bartolino *et al.*, 2011; Wood, 2017). Pairwise correlation plots were conducted, including all covariates in the models, and all correlation values between covariates were found to be ≤ 0.5. We note that YFS bottom depth and salinity covariates were correlated (>0.5) until YFS depths were constrained to <100 m. Partial effect plots were visually examined to confirm the biological realism of the models and were compared across species and life stages.

Models applied to the larval life stage included day of year (d, basis function behaviour restricted by setting the knot value (k) to 7), latitude (ϕ), longitude (λ), bottom depth (b, basis function behaviour restricted by setting k to 5), and year as a factor variable (yr) as covariates (Leathwick *et al.*, 2006). Longitude and latitude were interacted with one another through a thin plate regression spline to produce a two-dimensional smoother. The SST and SSS partial effects, in larval models, were restricted by constraining the basis functions' k value to 4 for all models. In the bivariate model [equation (5)], this resulted in a k constraint of 16. Models applied to the egg life stage included day of year (d; note that basis function behaviour of this covariate in egg models was not constrained), latitude (ϕ), longitude (λ), bottom depth (b, basis function behaviour restricted by setting k to 5), regional temperature index ($reg.SST$), and year as a factor variable (yr) as covariates. Longitude and latitude were also interacted through a thin plate regression spline. The addition of years into GAMs for both life stages helps to account for interan-

Table 3. Description of spatial and temporal attributes of ichthyoplankton data after trimming modifications (eggs and larvae) and pairing with *in situ* environmental data (larvae).

Species	Life stage	Geographic range	Depth range (m)	Detailed seasonality (day of year)/Years sampled	Number of stations sampled/Number of stations sampled with positive catches
Alaska plaice	Egg	53.98 to 62.2°N, 158.24 to 178.35°W	19–150	100–181/1979, 1988, 1991, 1993–2000, 2002, 2003, 2005–2016	1963/798
Alaska plaice	Larvae	54.28 to 59.72°N, 158.24 to 173.02°W	23–150	99–175/1997–2000, 2002, 2003, 2005–2016	955/225
Flathead sole	Egg	53.50 to 60.1°N, 159.4 to 178.35°W	24–220	100–174/1979, 1988, 1991, 1993–2000, 2002, 2003, 2005–2016	2020/1017
Flathead sole	Larvae	54.00 to 59.14°N, 158.86 to 173.5°W	24–220	100 to 174/1997–2000, 2002, 2003, 2005–2016	1273/405
Northern rock sole	Larvae	53.37 to 59.73°N, 158.63 to 178.17°W	41–298	101–159/1997–2000, 2002, 2003, 2005–2016	1247/630
Pacific cod	Larvae	53.39 to 59.64°N, 158.86 to 178.17°W	43–232	100–159/1997, 1998–2000, 2002, 2003, 2005–2016	915/258
Walleye pollock	Egg	54.00 to 60.08°N, 158.24 to 173.00°W	0–3 480	100–159/1979, 1988, 1991–2000, 2002, 2003, 2005–2016	2504/1997
Walleye pollock	Larvae	53.65 to 60.08°N, 158.24 to 174.04°W	24–3 365	99–159/1997–2000, 2002, 2003, 2005–2016	1584/1143
Rex sole	Egg	53.36 to 58.35°N, 161.59 to 172.91°W	0–3 242	91–212/1979, 1988, 1991–2016	1907/328
Yellowfin sole	Larvae	54.95 to 65.00°N, 158.06 to 171.23°W	16–93	231–281/2000, 2004–2006, 2008–2016	369/188

All ichthyoplankton data were modified by geographic, temporal, and depth values to align with species' life history characteristics; stations were also removed if farther than 30 km from any positive catch of that species. These data were retrieved from AFSC EcoFOCI Ichthyoplankton Records.

nual variation in ichthyoplankton abundance due to interannual variation in spawning stock population size.

The response variable (μ) was catch (of eggs or larvae) per 10 m^2 + 1, and models were fitted on a Tweedie distribution with a natural log link function. The log link function applies a log transformation to the linear predictor, while leaving the response variable untransformed. This method was applied to ensure that linear predictors of these models align with the distribution of the observations, as larval data were significantly overdispersed and zero-inflated. All models were applied to untransformed data. Note that in the model equation syntax, we adopt the convention that μ is the linear predictor (i.e. not the observed value) and the response is in the scale of the link function. When using the Tweedie distribution, the link function is the natural log. Random error (ϵ) is assumed to occur over a Tweedie distribution, and the variance is defined by $\vartheta(\mu_{d,yr,(\phi,\lambda)}) = \varphi \cdot \mu_i^p$, where p is equal to the Tweedie parameter ranging from one (Poisson distribution) to two (Gamma distribution).

The best-performing model for each species was selected by comparing Akaike Information Criterion (AIC) scores and retaining the model with the smallest AIC value (Akaike, 1974; Burnham and Anderson, 2004).

Larval models

In the larval models, all covariates were included additively; the individual covariates' effects on larval catch do not depend on the values of any other covariate. The base model formulation [equation (1)] lacked any inclusion of environmental parameters.

$$log(\mu_{d,yr,(\phi,\lambda)}) = factor(yr) + s_1(d,\ k = 7) + g_1(\lambda,\phi) + s_2(b_{\phi,\lambda},\ k = 5). \quad (1)$$

The next two model formulations included *in situ* sea surface salinity [*SSS*; equation (2)] and *in situ* sea surface temperature [*SST*; equation (3)] as additive covariates:

$$log(\mu_{d,yr,(\phi,\lambda)}) = factor(yr) + s_1(d,\ k = 7) + g_1(\lambda,\phi) + s_2(b_{\phi,\lambda},\ k = 5) + s_3(SSS_{b,\phi,\lambda,d},\ k = 4), \quad (2)$$

$$log(\mu_{d,yr,(\phi,\lambda)}) = factor(yr) + s_1(d,\ k = 7) + g_1(\lambda,\phi) + s_2(b_{\phi,\lambda},\ k = 5) + s_3(SST_{b,\phi,\lambda,d},\ k = 4). \quad (3)$$

We then included *SST* and *SSS* together, additively [equation (4)]. In the final model formulation, *SST* and *SSS* were interacted together in one interaction [equation (5)]; in this formulation, the effect of *SST* on larval catch depends on the value of *SSS*, and vice versa:

$$log(\mu_{d,yr,(\phi,\lambda)}) = factor(yr) + s_1(d,\ k = 7) + g_1(\lambda,\phi) + s_2(b_{\phi,\lambda},\ k = 5) + s_3(SSS_{b,\phi,\lambda,d},\ k = 4) + s_4(SST_{b,\phi,\lambda,d},\ k = 4), \quad (4)$$

$$log(\mu_{d,yr,(\phi,\lambda)}) = factor(yr) + s_1(d,\ k = 7) + g_1(\lambda,\phi) + s_2(b_{\phi,\ \lambda},\ k = 5) + g_2(SSS_{b,\ \phi,\lambda,d}, SST_{b,\ \phi,\lambda,d},\ k = 16). \quad (5)$$

Once fitted and selected, larval catch estimates [log (catch per 10 m^2 + 1)] were predicted over a regularly spaced grid of longitude and latitude by the best-performing model to visualize the results and spatial distribution. Similarly, species' larval catch was also predicted over a regularly spaced SSS–SST grid to visualize the distribution over environmental coordinates. Additionally, larval catches were subset to include only 65% of the sum of estimated larval catches for each species to ascertain where in SSS–SST space the majority of estimations occurred. In addition to the model AIC, outputs were qualitatively validated by comparing estimates with observed larval catch.

Egg models

In the base model [equation (6)], all dimensions and variables are included additively, wherein the specific effects of covariates on egg catch do not depend on the values of other covariates:

$$log(\mu_{d,yr,(\phi,\lambda)}) = factor(yr) + s_1(d) + s_2(b_{\phi,\ \lambda},\ k = 5) + g_1(\lambda,\phi). \quad (6)$$

We then formulated variable-coefficient GAMs (vGAMs; e.g. Bacheler *et al.*, 2009, 2012; Bartolino *et al.*, 2011); these are formulations in which the response variable (μ) is modelled with the inclusion of a term representing either phenology [equation (7)] or geography [equation (8)] that varies in relation to the regional temperature index (*reg.SST*, °C):

$$log(\mu_{d,yr,(\phi,\lambda)}) = factor(yr) + s_1(d) \times reg.SST + s_2(b_{\phi,\ \lambda}, k = 5) + g_1(\lambda,\phi), \quad (7)$$

$$log(\mu_{d,yr,(\phi,\lambda)}) = factor(yr) + s_1(d) + s_2(b_{\phi,\ \lambda}, k = 5) + g_1(\lambda,\phi) \times reg.SST. \quad (8)$$

We finally formulated threshold GAMs (tGAMs); these are formulations in which the response variable (μ) is modelled with the inclusion of a term that specifies a threshold regional sea surface temperature index (e.g. Ciannelli *et al.*, 2004; Porter and Ciannelli, 2018). The response variable is then modelled differently above and below this threshold temperature in either time [equation (9)] or space [equation (10)]. In these formulations, I is an indicator variable (between 0 and 1) that relates to whether the regional temperature index is above or below the threshold:

$$log(\mu_{d,yr,(\phi,\lambda)}) = factor(yr) + I_1 s_1(d) + I_2 s_2(d) + s_3(b_{\phi,\ \lambda}, k = 5) + g_1(\lambda,\phi), \quad (9)$$

$$log(\mu_{d,yr,(\phi,\lambda)}) = factor(yr) + s_1(d) + s_2(b_{\phi,\ \lambda}, k = 5) + I_1 g_1(\lambda,\phi) + I_2 g_2(\lambda,\phi). \quad (10)$$

The best threshold temperature, for each species, was chosen by iteratively fitting models with 39 different unique threshold temperatures and selecting the temperature that produced the model with the lowest AIC score (Akaike, 1974; Burnham and Anderson, 2004).

For the egg models, mean squared error (MSE) reduction was also determined by comparing the MSE% reduction obtained from the threshold geography model [equation (10)], relative to the base model, and the threshold phenology model [equation (9)], relative to the base model. MSE% reduction was calculated by subtracting the MSE of the best model from the MSE of the base model and dividing that value by the MSE of the base model. The percentage reduction of MSE can help inform whether there is a trade-off in shifting spawning behaviour in space or time.

Model outputs were created using the *mgcv* package in *R* [version 4.1.0 (2021–5–18) and *mgcv* package version 1.8–35] and validated by comparing outputs to observed egg catches. Spatially varying predictions of egg catch, as estimated by either a tGAM or vGAM, were visualized over a regularly spaced longitude and latitude grid.

Results

Sea surface salinity and temperature

In warm years, May sea surface temperature (SST) was homogenous across the southeastern BS with little variation across domains (Supplementary Information Section 3). SST values were ~6°C across most of the shelf, with some pockets of higher (7–8°C) temperatures observed. Cold SSTs (<4°C) were restricted to latitudes >58°N within the middle domain. Sea surface salinity (SSS) patterns were consistent with the long-term average conditions, with the freshest water occurring close to the Alaska coasts (between 30 and 31) and SSS values increasing with distance offshore (between 32.5 and 33.5). In September, the data available show SST values in the middle domain ranging from ~8 to 11°C, with warmer SST in shallower areas. September SSS was similar to the long-term average conditions, with values ranging between 31 and 32 in the middle domain and 32 and above in the outer domain. Fresher values also occurred towards the northern limits of the study region, near the 60°N line (Supplementary Information Section 3).

In cold years, May SST was more variable across the shelf, with the coldest temperatures (<0°C) occurring in the middle domain (Supplementary Information Section 3). SSTs warmed with distance offshore, reaching values ~4°C in the outer domain and along the southern Aleutian Islands. May SSS patterns were roughly inverse to this, with saltiest (33.5) water occurring in the outer domain and fresher water (31–32) occurring in the middle domain. In September, data showed warmer SST (9–10°C) in the coastal domain and the middle domain, ranging from 5 to 8°C. September SSS were fresher in the middle domain than during warm years and long-term average conditions; in the middle domain, values were between 31 and 31.5, with fresher SSS occurring in the coastal domain and saltier SSS (>32) occurring in the outer domain (Supplementary Information Section 3).

In May, the middle domain retained some cooler SST even in warm years, while the coastal and outer domains were consistently warmer than in cold regime years (Figure 2). In September, SST and SSS observations do not suggest distinct patterns between warm and cold regime years. Warmest and freshest sea surface conditions occurred in the coastal domain in May across both cold and warm regimes. In September, the

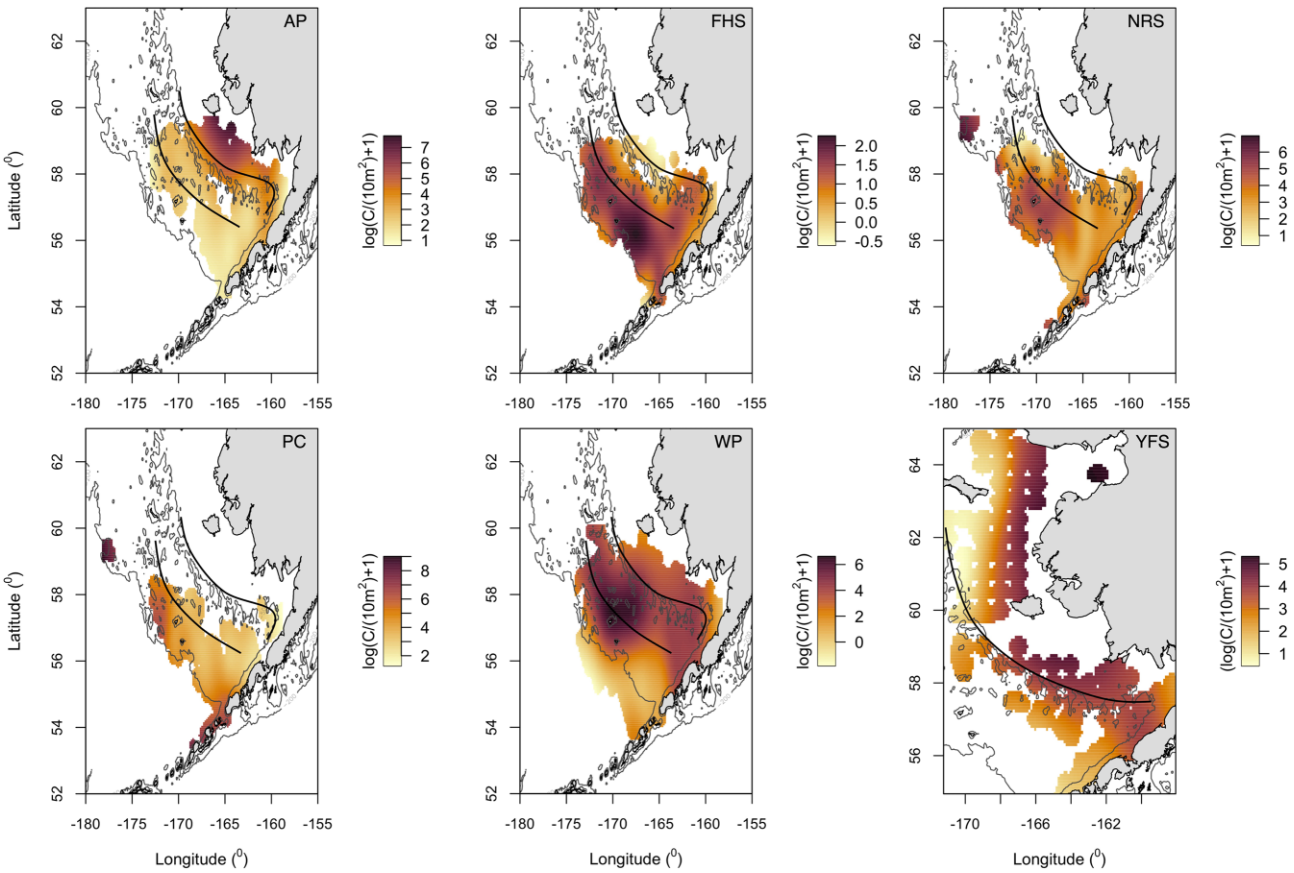

Figure 3. Biogeography of larval species as estimated by the best-performing models for each species: Alaska plaice (AP), flathead sole (FHS), northern rock sole (NRS), Pacific cod (PC), walleye pollock (WP), and yellowfin sole (YFS). Overlaid black lines indicate general boundaries of the coastal domain (depths < 50 m) and the middle domain (depths > 50 m and < 100 m) for reference.

warmest and freshest conditions also occurred in the coastal domain across both regimes (Figure 2).

Larval environmental associations

Alaska plaice, flathead sole, northern rock sole, Pacific cod, and walleye pollock larvae were caught between day 100 (10 April) and day 180 (29 June); yellowfin sole (YFS) catches occurred later in the season, from day 231 (19 August) to day 281 (8 October; Table 3). The predicted average distributions of all larvae are shown in Figure 3. To view the spatial distributions of observed larval log (catch per 10 m^2), see Supplementary Information Section 5.

The model with an interaction between *in situ* SSS and SST [equation (5)] best estimated catches of Alaska plaice (AP; 80.9% deviance explained), flathead sole (FHS; 79.1% deviance explained), northern rock sole (NRS; 63.5% deviance explained), Pacific cod (PC; 69% deviance explained), walleye pollock (WP; 62.8% deviance explained), and yellowfin sole (YFS; 69.2% deviance explained; Table 4). While the difference in deviance explained by the best-performing models compared to other tested models for each species was modest, it was paired with a substantial improvement to AIC values (Table 4).

All best-performing models included a phenology term, which indicates the estimated seasonality of each larval species (Supplementary Information Section 5). The best-performing models estimated a linearly positive phenology curve for AP, NRS, and YFS, with the greatest effect of day of year on larval catch later in the season (AP: day ~180, NRS: day ~160, YFS: day ~280). The best-performing models estimated more dynamic phenology curves for FHS, PC, and WP (Supplementary Information Section 5).

Predicted geographic distributions of larvae varied across species and were heterogenous across the southeastern BS region (Figure 3). AP predicted larval catches predominately occurred in the coastal domain north of Bristol Bay, with catches decreasing with distance offshore. YFS-predicted larval catches followed a similar pattern, with the greatest predictions occurring in the coastal domain. The highest predicted YFS larval catches occurred north of Nunivak Island. FHS and PC estimates of larval catches occurred primarily in the outer domain. WP and NRS estimates of larval catches occurred primarily in the middle domain, though both species had estimated catches in the coastal and outer domains as well (Figure 3).

When larval catch was predicted on an SST–SSS grid, AP, FHS, NRS, PC, and WP catches were distributed roughly between −1.6 and 8°C and between 30 and 33 (Figure 4, greyscale). YFS occupied space diverged from the other species, with estimated catches spanning 29–32 salinity and 2.5–14°C. When investigating the bivariate space in which 65% of catch estimates occurred for each species (Figure 4, colour-scale), AP, NRS, PC, and YFS were found at the lower respective

Table 4. Model output values and ΔAIC scores (difference in AIC relative to the best-performing model, wherein a higher value indicates a worse-fitting model) for all tested larval models [equations (1) through (5)].

	Model	Deviance explained (%)	Significance codes of covariates (effective degrees of freedom)	ΔAIC
Alaska plaice	Base [1]	77.4		117.88
	Additive SSS [2]	77.4		119.12
	Additive SST [3]	78.7		49.68
	Additive SSS and SST [4]	78.8		51.96
	Bivariate SSS, SST [5]	*80.9*	*DOY*** (1.00), BD** (3.61), LON/LAT*** (24.47), SSS/SST***(32.21)*	-
Flathead sole	Base [1]	72.4		282.75
	Additive SSS [2]	72.5		277.87
	Additive SST [3]	74.4		177.46
	Additive SSS and SST [4]	74.5		182.91
	Bivariate SSS, SST [5]	*79.1*	*DOY*** (5.10), BD. (1.95), LON/LAT*** (23.47), SSS/SST*** (59.7)*	-
Northern rock sole	Base [1]	50.7		340.58
	Additive SSS [2]	52.2		294.57
	Additive SST [3]	54.3		224.30
	Additive SSS and SST [4]	55.1		205.29
	Bivariate SSS, SST [5]	*63.5*	*DOY* (1.00), BD*** (7.28), LON/LAT*** (26.30), SSS/SST*** (56.04)*	-
Pacific cod	Base [1]	60.6		141.76
	Additive SSS [2]	60.9		138.97
	Additive SST [3]	60.6		143.22
	Additive SSS and SST [4]	61.4		130.43
	Bivariate SSS, SST [5]	*69*	*DOY** (4.99), BD* (1.41), LON/LAT*** (23.94), SSS/SST***(49.34)*	-
Walleye pollock	Base [1]	50.7		429.17
	Additive SSS [2]	52.9		335.46
	Additive SST [3]	57.1		147.67
	Additive SSS and SST [4]	57.5		138.77
	Bivariate SSS, SST [5]	*62.8*	*DOY*** (4.38), BD (1.51), LON/LAT*** (27.19), SSS/SST*** (61.54)*	-
Yellowfin sole	Base [1]	60.1		54.24
	Additive SSS [2]	61.9		36.64
	Additive SST [3]	62.5		27.52
	Additive SSS and SST [4]	64.5		9.91
	Bivariate SSS, SST [5]	*69.2*	*DOY (1.00), BD*** (3.92), LON/LAT*** (19.37), SSS/SST*** (24.96)*	-

Effective degrees of freedom are included in parentheses for all covariates. The best-performing model is italicized for each species, and significance of covariates (day of year (DOY), bottom depth (BD), latitude and longitude (LON/LAT), sea surface salinity (SSS), sea surface salinity (SST), bivariate sea surface salinity and temperature (SSS/SST)) within the best-performing model are provided. Significance codes: "***" < 0.001, "**" < 0.01, "*" < 0.05, "."< 0.1.

ranges of salinity (between 30 and 31), whereas FHS and WP were found at middle to higher salinity ranges (between 31 and 33). AP and WP had highest catch estimates across a relatively small range of moderate temperatures (AP: 3.66–6.28°C; WP: 3.97–6.18°C for WP). NRS and PC had highest catch estimates across a larger range of low to moderate temperatures (NRS: 1.37–6.79°C; PC: 0.58–7.91°C). FHS and YFS had highest catch estimates at higher temperatures, with high YFS predictions occurring at the warmest temperatures of these species (FHS: 5.24–8.04°C; YFS: 9.07–12.15°C).

Evaluation of spawning behaviour

Eggs of most species were caught between day 100 and day 180; however, rex sole (RS) positive catches were protracted, occurring from day 91 to day 212 (31 July; Table 3). Egg catches for all four species were best estimated by threshold models [tGAMs; equation (10)], which included geographic flexibility (Table 5). The tGAMs identified unique temperature thresholds of 2.18°C for AP (74.8% deviance explained), 2.33°C for FHS (59.8% deviance explained), 2.31°C for RS (61.2% deviance explained), and 2.08°C for WP (58.8% deviance explained). The improvement in perfor-

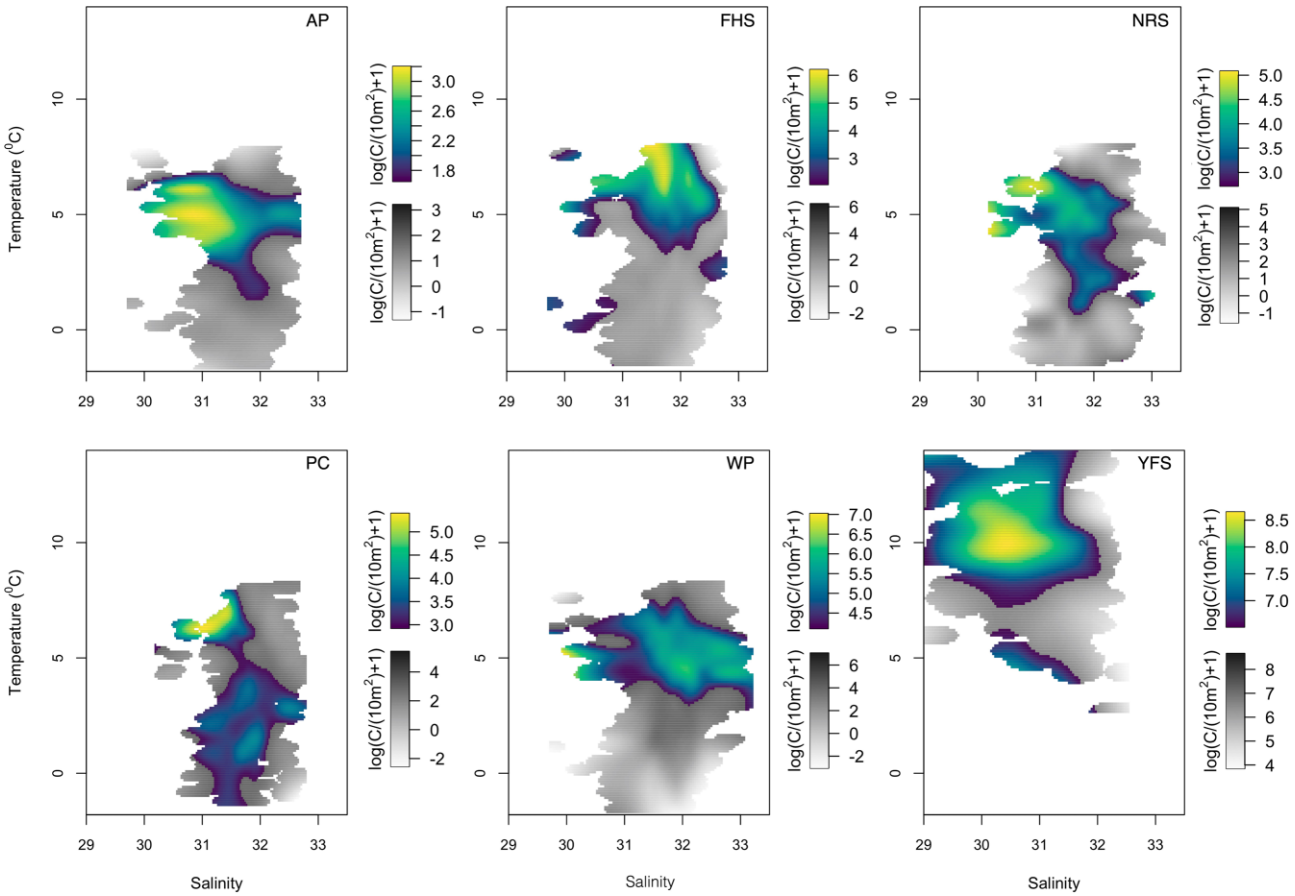

Figure 4. Sea surface salinity-temperature plots, as predicted by the best-fitting GAM, for each of the six larval species: Alaska plaice (AP), flathead sole (FHS), northern rock sole (NRS), Pacific cod (PC), walleye pollock (WP), and yellowfin sole (YFS). Coloured scale reflects the region in salinity-temperature space in which 65% of total predicted log (catch per 10 m^2 + 1), lies while the grey scale reflects all predicted log (catch per 10 m^2 + 1).

mance made by this formulation is also reflected in improved (i.e. smaller) AIC scores (Table 5).

Spatially explicit estimates of egg abundance above (warmer conditions) and below (colder conditions) the threshold temperature varied by species, but each species demonstrated areas of increased egg abundance in conjunction with a transition to warmer conditions (Figure 5). AP egg abundance increased west of Nunivak Island, and WP egg abundance increased southwest of Nunivak Island in warmer conditions. FHS egg abundance increased south of Bristol Bay in the coastal and middle domains, and increased egg catches were also estimated west of Nunivak Island in the outer domain. RS egg abundance increased southwest of Unimak Pass in warmer conditions (Figure 5).

Spawning phenology, as estimated by the tGAMs for each species, varied across species (Supplementary Information Section 6). WP and RS models demonstrated the greatest day of year effect, with WP peaking slightly after day 120 and RS peaking at roughly day 170. RS and AP exhibited multiple positive anomalies in the phenology response curves. FHS exhibited a positively sloping day of year effect from day 100 to roughly day 125; this effect levelled off and intersected with zero at roughly day 170 (Supplementary Information Section 6).

Comparisons of % MSE difference across threshold geography and threshold phenology, both relative to the base model, suggested trade-offs in flexibility for all study species (Table 5). All study species demonstrated a larger % MSE reduction with threshold geography than threshold phenology (AP = Δ12.6%; FHS = Δ5.75%; RS = Δ14.8%; WP = Δ11.1%, where Δ = % MSE $\text{reduction}_{\text{threshold geography}}$—% MSE $\text{reduction}_{\text{threshold phenology}}$).

Discussion

We examined the flexibility of groundfish egg and larval habitat associations as well as the seasonal patterns of production in seven species with contrasting life history strategies. We found evidence that AP, FHS, WP, and RS can exhibit geographic flexibility in their spawning behaviour, as egg distributions for all species were best explained by a model that allowed for interannual modifications in spatial distributions across a sea surface temperature threshold (Table 5). Additionally, there appeared to be a trade-off in spawning behaviour flexibility; all species demonstrated a larger % MSE reduction in models with geographic flexibility than phenologic flexibility (Table 5). This is consistent with the notion that species may be flexible but only in one dimension: either space or time. Our results indicate that these species may continue to exhibit shifts in their spatial distributions of spawning as the BS warms past the respective SST thresholds identified. These species may also be more constrained in the time at which they spawn.

Table 5. Model output values and validation scores (ΔAIC (difference in AIC relative to the best performing model) and mean square error (MSE) difference (%; difference in MSE relative to the base model) for all tested egg models [equations (6) through (10)].

	Model	Deviance explained (%)	Significance codes of covariates (effective degrees of freedom)	ΔAIC	MSE difference (%)
Alaska plaice	Base [6]	69.1		444.00	-
	V-C Phenology [7]	70.3		369.18	2.85
	V-C Geography [8]	73.6		116.21	11.77
	Threshold Phenology [9]	70.2		315.81	2.81
	Threshold Geography [10]	*74.8*	*DOY*** (8.01), BD*** (3.92), LON/LAT$_B$*** (27.59), LON/LAT$_A$*** (26.69)*	-	*15.39*
Flathead sole	Base [6]	54.2		289.59	-
	V-C Phenology [7]	56		205.40	3.18
	V-C Geography [8]	58.9		56.65	8.28
	Threshold Phenology [9]	56.6		171.77	4.26
	Threshold Geography [10]	*59.8*	*DOY*** (5.72), BD (3.92), LON/LAT$_B$*** (27.59), LON/LAT$_A$***(19.21)*	-	*10.01*
Rex sole	Base [6]	50.8		454.13	-
	V-C Phenology [7]	52.3		414.87	2.56
	V-C Geography [8]	56.5		202.40	10.06
	Threshold Phenology [9]	52.8		389.57	3.59
	Threshold Geography [10]	*61.2*	*DOY*** (8.45), BD*** (3.58), LON/LAT$_B$*** (25.12), LON/LAT$_A$*** (26.00)*	-	*18.38*
Walleye pollock	Base [6]	50.2		593.08	-
	V-C Phenology [7]	52.2		465.06	3.27
	V-C Geography [8]	57.7		75.96	12.49
	Threshold Phenology [9]	52.1		469.11	3.17
	Threshold Geography [10]	*58.8*	*DOY*** (7.23), BD*** (1.25), LON/LAT$_B$*** (27.97), LON/LAT$_A$*** (27.21)*	-	*14.30*

Effective degrees of freedom are included in parentheses for all covariates. The best-performing model is italicized for each species, and significance of covariates [day of year (DOY), bottom depth (BD), latitude and longitude below threshold (LON/LAT$_B$), and latitude and longitude above threshold (LON/LAT$_A$) within the best-performing model are provided]. Significance codes: "***" < 0.001, "**" < 0.01, "*" < 0.05, "."< 0.1.

The improvement in deviance explained between the base model (longitude, latitude, bottom depth, and day of year as covariates) and the best-performing model were moderate. This is not surprising, considering that these species do tend to spawn in predictable areas and at predictable times. These results are thus consistent with ecology of the species and the known importance of space and time. However, the inclusion of environmental variables in these models provides evidence of the importance of additional factors (i.e., those other than space and time) in the spawning habitat, and such factors are likely essential to correctly model future species distributions under continuous global change.

In 2012, Bacheler *et al.* (2012) analysed WP data sourced from the EcoFOCI programme and identified consistent inter-annual spawning behaviour in space and time, though temperature appeared to modify the magnitude of egg production. With the added advantage of a decade of WP data, including some of the warmest years on record for the region, this study augmented Bacheler *et al.*'s findings and suggests that WP may exhibit more apparent northward movements in spawning aggregations in the future (Figure 5). FHS phenology and geography were also recently analysed by Porter and Ciannelli (2018); this study looked only at spatially variable spawning behaviour and found that FHS exhibit a northeastward shift in spawning habitat in relation to warming temperatures, but their sampled area was limited to the Alaska peninsula. FHS egg distributions in the present study increased southeast of the Pribilof Islands in relation to warmer conditions (Figure 5); considering the difference in spatial domain, this finding is consistent with those of Porter and Ciannelli (2018). To date, studies have not been conducted for AP and RS in the BS. Trends of spawning flexibility observed in the literature (see Sims *et al.*, 2004; Asch, 2015; McQueen and Marshall, 2017; Rogers and Dougherty, 2019; Slesinger *et al.*, 2021) and this study suggest a wider spread of behavioural flexibility than previously recognized for iteroparous marine fish.

There are many possible explanations for underlying drivers of geographic flexibility patterns. FHS and RS are at the northern edge of their range in the BS, which may make them more responsive to unfavourable variations in temperature (Matarese *et al.*, 2003; Porter and Ciannelli, 2018). Consistently, for both of these species, the respective best-performing model predicted lower catches in the middle domain and a northward shift with warmer temperatures (Figure

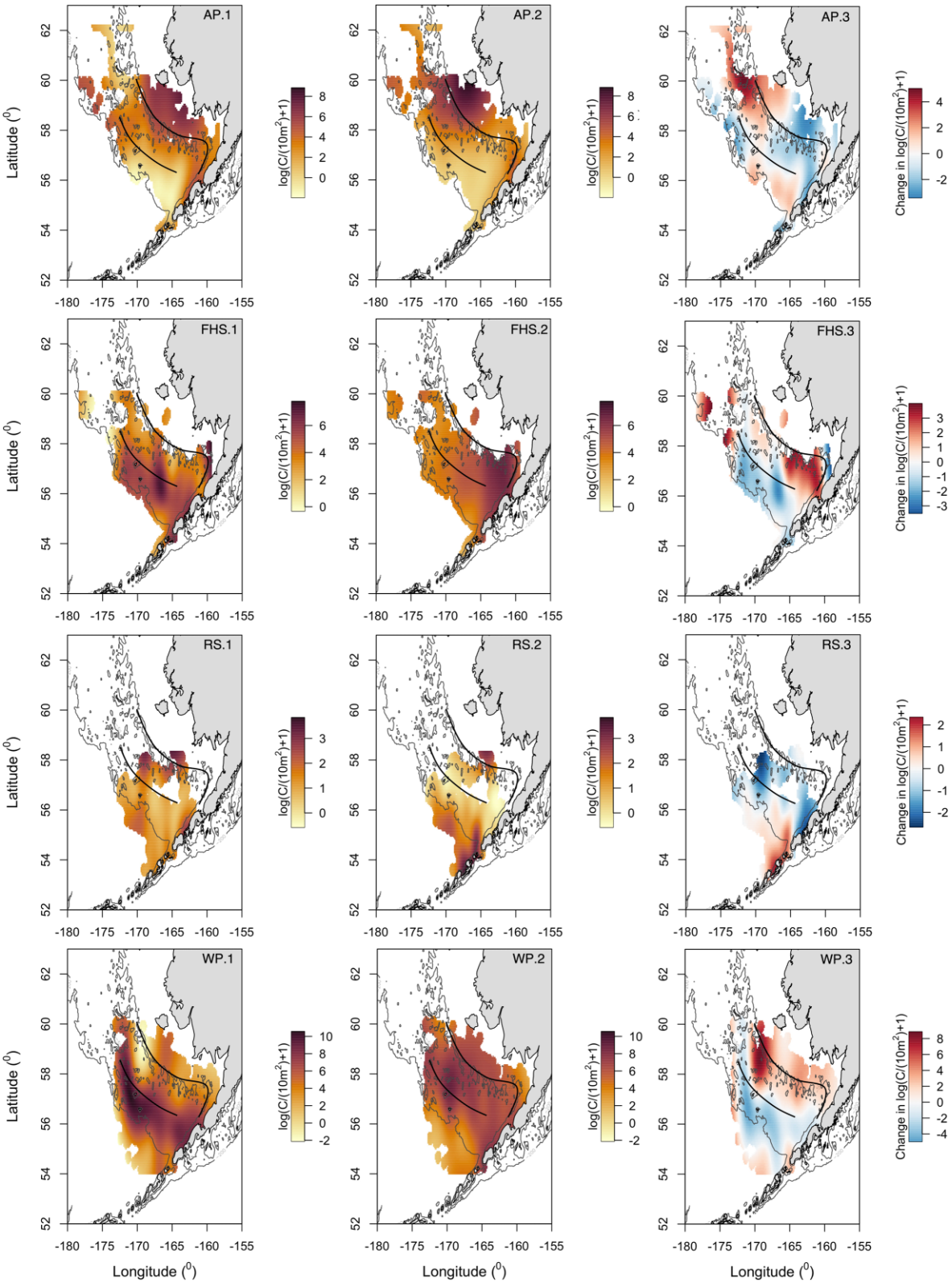

Figure 5. Spatial distributions of egg catch [log (catch per 10 m^2 + 1)] estimates by threshold geography GAMs below (1) and above (2) the temperature threshold for Alaska plaice (AP), flathead sole (FHS), rex sole (RS), and walleye pollock (WP). Additionally, changes in distribution of egg catch estimates about the temperature threshold (3) are shown for each species. More positive values in this panel indicate regions where estimated egg catches were greater above the temperature threshold (i.e. in warmer conditions) than below the threshold. Overlaid black lines indicate general boundaries of the coastal domain (depths < 50 m) and the middle domain (depths > 50 m and < 100 m) for reference.

5). Differences in the shelf location where increased egg catch estimates occur across species may be related to fine-scale differences in spawning migrations, egg buoyancy properties, or fine-scale retention features like eddies and fronts. However, the dispersal pathways utilized by all species here are relatively broad-scale features across the BS shelf, which suggests that geographic modifications to spawning grounds may still allow the transport of eggs and larvae to favourable habitats (Pearcy *et al.*, 1977; Bailey *et al.*, 2003; Petrik *et al.*, 2016; Porter and Ciannelli, 2018). AP and WP both migrate to inshore or on-shelf areas to spawn; this reproductive strategy may explain the observed northward shift in egg catch estimates during warmer conditions as they appear to follow environmental cues for the onset of spawning migration (Bailey *et al.*, 2003; Matarese *et al.*, 2003; Petrik *et al.*, 2016).

Our results suggest that these study species can exhibit plasticity in where they spawn, though variations in advective processes between warm and cold years in the BS could also lead to differential distributions of eggs. The BS has exhibited patterns of heightened advection of water northwards into the Chukchi Sea in recent warmer years (Spear *et al.*, 2020); such advection could be the driver of egg displacement north of historic spawning grounds in warm years, as seen with AP, FHS, WP, and RS in this study. Advection was not studied in the present analysis and thus represents a caveat with our findings. Additionally, we detected a greater flexibility in spawning geography than in phenology. The surveys we used to estimate egg and larval abundance and distribution may not be well suited to estimate changes in phenology because they tend to occur once a year over a limited time window. In aggregate, however, they span a larger seasonal window. Furthermore, regional temperature does have direct effects on spawning adults as their thermal tolerance is narrowed during reproduction and gonadal development is temperature-dependent; we could not evaluate this in our study (Servili *et al.*, 2020). Despite these caveats to our findings, it is reasonable to conclude that our results regarding spawning behaviour are useful to further conceptualize the response that species may exhibit in the future.

The six species analysed here for larval biogeography—AP, FHS, NRS, PC, WP, and YFS—exhibited species-specific SST and SSS associations (Figure 4). Similar to what we have discussed for egg stages, larvae are also known to inhabit ecosystems at predictable times and locations, so it is not surprising that the base models capture most of the variability, leading to modest improvements in deviance explained in the best-performing models. However, even these modest gains in deviance explained by models with environmental variables have biological significance, especially in light of forecasting species distributions, because they inform how predictions can be made about the degree to which larvae will track future environmental conditions.

The patterns of SSS and SST across warm and cold years, as well as the projections of physical change in the BS from other recent studies (Hermann *et al.*, 2019; Ciannelli *et al.*, 2022b), suggest that larval exposure to potentially unfavourable habitats may occur through all three hydrographic domains. The coastal shelf will likely experience the greatest seasonal change in SST and SSS, which could impact the growth and development of YFS and AP (Ciannelli *et al.*, 2022b). However, the middle and outer shelves also demonstrated substantial changes in May SST between warm and cold years (Figure 2). Such changes could also impact the growth and development of the other four species (FHS, NRS, PC, and WP), as larval growth is closely temperature-dependent. Additionally, SSS decreases in the middle domain in warm conditions, which could also impact the growth and survivability of WP, FHS, and NRS. The buoyancy of larvae and thus their ability to access prey at various vertical locations in the water column may also be impacted by salinity changes.

Climate change is and will continue to exert significant pressures on the sensitive early life stages of these species. Even minor variations in SST and SSS can exert significant physiological stress on early life stages or spawning adults, threatening their survivability in the future (Klein *et al.*, 2017; Dahlke *et al.*, 2020; Kim *et al.*, 2022; Ciannelli *et al.*, 2022a). Though, there could also be positive repercussions to such changes. In warm years, YFS were found to expand their spawning distributions and produce more larvae relative to cold years (Porter, 2021). These larvae may face additional impacts due to the increased seasonality of coastal SST and SSS conditions, but such impacts could be balanced by increased production (Porter, 2021; Ciannelli *et al.*, 2022b). However, the risk of larval production that is asynchronous with prey availability is significant under climate change, and the assemblages of prey species may shift towards less nutritious options in warmer conditions, increasing the likelihood of malnutrition and starvation in larvae (Hunt and Stabeno, 2002; Litzow *et al.*, 2006; Klein *et al.*, 2017).

WP and AP demonstrated northward shifts in spawning aggregations in warmer years, which may subsequently source larvae into northern middle and coastal shelf habitats. These two species had very similar SST and SSS associations (Figure 4), though the peak in WP larval catch estimates occurred at a slightly lower salinity (29.96) compared with AP (30.86). As previously mentioned, inshore SSS values are projected to decrease, which could impact the survivability of WP through increased physiological stress or buoyancy modifications on larvae or require colonization of new habitats (Bœuf and Payan, 2001; Hermann *et al.*, 2019). In contrast, the middle domain exhibited variance across warm and cold years that coincided with the range of SSTs associated with higher larval catch estimates for WP; this may allow for maintained WP larval growth despite a geographic northward shift to new nursery areas (Figures 2, 4, and 5). In warmer conditions, FHS egg catch abundance increased southwest of Bristol Bay in the coastal and middle domains north of Unimak Pass. FHS larval catch estimates were associated with a range of SSTs slightly warmer than WP; these associations suggest FHS could weather changing conditions in warmer years (Figures 2 and 4). Additionally, FHS larvae were recently found to exhibit a more robust life history strategy against climate change by occurring in deeper waters at earlier stages of life and migrating inshore with age (Ciannelli *et al.*, 2022a).

Coastal areas are projected to experience decreased salinity as a result of increased precipitation and advection modifications (Polyakov *et al.*, 2020; IPCC: Summary for Policymakers, 2022). Coastal areas represent important nursery habitats for the species of groundfish discussed in the present study as well as numerous other commercially important marine species (Lanksbury *et al.*, 2007; Siddon *et al.*, 2011; Petrik *et al.*, 2016). The suitability of thermohaline environments in coastal areas may be significantly altered in the coming decades, affecting these study species and other members of their ecosystem. The present study developed models that help untangle important drivers of plasticity and environmental as-

sociations, but future investigation is certainly warranted to clarify and synthesize the mechanistic drivers of patterns, the impacts of biological factors (temperature-dependent larval growth, predation, and prey availability), and the potential impacts of climate change to commercial fisheries and ecosystems.

Importantly, the fate of the Alaskan economy is intertwined with the species supporting its extremely valuable fisheries (e.g. YFS, WP, and PC). The economic viability and sustainable harvest potential of these fisheries, however, are unclear as climate change introduces sweeping impacts to the BS (O'Leary *et al.*, 2021). Alaskan fisheries management is based around an ecosystem-based fisheries management (EBFM) framework, which acknowledges the cumulative impacts that can threaten multiple ecosystem components and is effective at promoting resilient social-ecological systems. These policies and practices have directed effective management to maintain robust fishery populations for decades (Holsman *et al.*, 2020). Improved monitoring of vulnerable life stages, including an emphasis on multi-dimensional habitat preferences (e.g. temperature, salinity, and preferences through ontogeny), can facilitate EBFM and integrated ecosystem assessments (IEA; Levin *et al.*, 2009) by elucidating periods of high or low mortality. The present study developed models that help untangle important drivers of plasticity and environmental associations, but future investigation is certainly warranted to clarify the mechanistic drivers of patterns and the potential impacts of climate change to commercial fisheries and ecosystems. Additional work focused on synthesizing mechanistic ecosystem relationships between recruitment and early life stage survivorship into stock assessments (e.g., Ecosystem-Socioeconomic Profiles, Shotwell *et al.*, 2022) can help reduce the burden of uncertainty in fisheries management and provide regional actors with improved place-based knowledge to inform management strategies that benefit fish and fishing communities into the future.

Acknowledgements

The authors greatly appreciate three anonymous reviewers who provided invaluable comments that helped evolve this manuscript.

Supplementary data

Supplementary material is available at the *ICESJMS* online version of the manuscript.

Conflict of interest

The authors have no conflicts of interest to declare.

Author contributions

Conceptualization: L.C. and L.V.; Data curation: L.V. and L.R.; Formal analysis: L.V. and L.C.; Funding acquisition: L.C., L.R., L.V.; Project administration: L.C., L.R., L.V., and M.H.; Visualization: L.V. and R.H.; Writing—original draft: L.V.; Writing—review & editing: all authors.

Funding

This work was made possible by financial support from the North Pacific Research Board (NPRB Project #1909-A "Phenology and Geography of Marine Fish" to Lorenzo Ciannelli and Lauren Rogers, and Graduate Student Research Award 1987–1987 to Laura Vary). Additionally, Laura Vary was supported by an Oregon State University Ocean Ecology of Nekton research award. This research is contribution EcoFOCI-1030 to NOAA's Ecosystems and Fisheries-Oceanography Coordinated Investigations Program.

Data availability

The data and metadata used in these analyses are available through the DataONE online research repository at https://doi.org/10.24431/rw1k7do. Raw ichthyoplankton data and conductivity–temperature–depth data are also available online at https://github.com/varyl97/Varyetal2023_ICES_JMS. This repository also contains code documents (with brief comments) representative of processes and analyses conducted in this study.

References

Abookire, A. A., and Bailey, K. M. 2007. The distribution of life cycle stages of two deep-water pleuronectids, Dover sole (*Microstomus pacificus*) and rex sole (*Glyptocephalus zachirus*), at the northern extent of their range in the Gulf of Alaska. Journal of Sea Research, 57: 198–208.

Akaike, H. 1974. A new look at the statistical model identification. IEEE Transactions on Automatic Control, 19: 716–723.

Asch, R. G. 2015. Climate change and decadal shifts in the phenology of larval fishes in the California Current ecosystem. Proceedings of the National Academy of Sciences, 112: E4065–E4074.

Asch, R. G., Stock, C. A., and Sarmiento, J. L. 2019. Climate change impacts on mismatches between phytoplankton blooms and fish spawning phenology. Global Change Biology, 25: 2544–2559.

Bacheler, N. M., Ciannelli, L., Bailey, K. M., and Bartolino, V. 2012. Do walleye pollock exhibit flexibility in where or when they spawn based on variability in water temperature? Deep Sea Research Part II: Topical Studies in Oceanography, 65–70: 208–216.

Bacheler, N., Bailey, K., Ciannelli, L., Bartolino, V., and Chan, K. 2009. Density-dependent, landscape, and climate effects on spawning distribution of walleye pollock *Theragra chalcogramma*. Marine Ecology Progress Series, 391: 1–12.

Bailey, K. M., Brown, E. S., and Duffy-Anderson, J. T. 2003. Aspects of distribution, transport and recruitment of Alaska plaice (*Pleuronectes quadrituberculatus*) in the Gulf of Alaska and eastern Bering Sea: comparison of marginal and central populations. Journal of Sea Research, 50: 87–95.

Baker, M. R. 2021. Contrast of warm and cold phases in the Bering Sea to understand spatial distributions of Arctic and sub-Arctic gadids. Polar Biology, 44: 1083–1105.

Bartolino, V., Maiorano, L., and Colloca, F. 2011. A frequency distribution approach to hotspot identification. Population Ecology, 53: 351–359.

Bellier, E., Planque, B., and Petitgas, P. 2007. Historical fluctuations in spawning location of anchovy (*Engraulis encrasicolus*) and sardine (*Sardina pilchardus*) in the Bay of Biscay during 1967–73 and 2000–2004. Fisheries Oceanography, 16: 1–15.

Biggs, C. R., Heyman, W. D., Farmer, N. A., Kobara, S., Bolser, D. G., Robinson, J., Lowerre-Barbieri, S. K. *et al.* 2021. The importance of spawning behavior in understanding the vulnerability of exploited marine fishes in the U.S. Gulf of Mexico. PeerJ, 9: e11814.

Boeing, W. J., and Duffy-Anderson, J. T. 2008. Ichthyoplankton dynamics and biodiversity in the Gulf of Alaska: responses to environmental change. Ecological Indicators, 8: 292–302.

Bœuf, G., and Payan, P. 2001. How should salinity influence fish growth? Comparative Biochemistry & Physiology Part C: Toxicology and Pharmacology 130: 411–423.

Boone, W., Rysgaard, S., Carlson, D. F., Meire, L., Kirillov, S., Mortensen, J., Dmitrenko, I. *et al.* 2018. Coastal freshening prevents fjord bottom water renewal in northeast Greenland: a mooring study from 2003 to 2015. Geophysical Research Letters, 45: 2726–2733.

K. P. Burnham, and D. R. Anderson (Eds). 2004. Model Selection and Multimodel Inference. Springer, New York, NY. http://link.springer.com/10.1007/b97636(last accessed 9 April 2023).

Ciannelli, L., Bailey, K. M., Chan, K. S., and Stenseth, N. Chr. 2007. Phenological and geographical patterns of walleye pollock (*Theragra chalcogramma*) spawning in the western Gulf of Alaska. Canadian Journal of Fisheries and Aquatic Sciences, 64: 713–722.

Ciannelli, L., Bailey, K., and Olsen, E. M. 2015. Evolutionary and ecological constraints of fish spawning habitats. ICES Journal of Marine Science, 72: 285–296.

Ciannelli, L., Chan, K.-S., Bailey, K. M., and Stenseth, N. Chr. 2004. Nonadditive effects of the environment on the survival of a large marine fish population. Ecology, 85: 3418–3427.

Ciannelli, L., Neuheimer, A. B., Stige, L. C., Frank, K. T., Durant, J. M., Hunsicker, M., Rogers, L. A. *et al.* 2022. Ontogenetic spatial constraints of sub-arctic marine fish species. Fish and Fisheries, 23: 342–357.

Ciannelli, L., Smith, E., Kearney, K., Hunsicker, M., and McGilliard, C. 2022. Greater exposure of nearshore habitats in the Bering Sea makes fish early life stages vulnerable to climate change. Marine Ecology Progress Series, 684: 91–102.

COBE SST: NOAA Physical Sciences Laboratory. 2005. https://psl.noaa.gov/data/gridded/data.cobe.html(last accessed 21 April 2021).

Cushing, D. H. 1990. Plankton production and year-class strength in fish populations: an update of the match/mismatch hypothesis. *In* Advances in Marine Biology, pp. 249–293. Ed. by J. H. S. Blaxterand and A. J Southward. Academic Press, Cambridge, MA.

Dahlke, F. T., Wohlrab, S., Butzin, M., and Portner, H. O. 2020. Thermal bottlenecks in the life cycle define climate vulnerability of fish. Science, 369: 65–70.

Dávila, P. M., Figueroa, D., and Müller, E. 2002. Freshwater input into the coastal ocean and its relation with the salinity distribution off austral Chile (35–55°S). Continental Shelf Research, 22: 521–534.

Doyle, M. J., Picquelle, S. J., Mier, K. L., Spillane, M. C., and Bond, N. A. 2009. Larval fish abundance and physical forcing in the Gulf of Alaska, 1981–2003. Progress in Oceanography, 80: 163–187.

Duffy-Anderson, J. T., Busby, M. S., Mier, K. L., Deliyanides, C. M., and Stabeno, P. J. 2006. Spatial and temporal patterns in summer ichthyoplankton assemblages on the eastern Bering Sea shelf 1996–2000. Fisheries Oceanography, 15: 80–94.

Duffy-Anderson, J. T., Doyle, M. J., Mier, K. L., Stabeno, P. J., and Wilderbuer, T. K. 2010. Early life ecology of Alaska plaice (*Pleuronectes quadrituberculatus*) in the eastern Bering Sea: seasonality, distribution, and dispersal. Journal of Sea Research, 64: 3–14.

Durant, J., Hjermann, D., Ottersen, G., and Stenseth, N. 2007. Climate and the match or mismatch between predator requirements and resource availability. Climate Research, 33: 271–283.

Folland, C. K., and Parker, D. E.. 1995. Correction of instrumental biases in historical sea surface temperature data. Quarterly Journal of the Royal Meteorological Society, 121: 319–367.

Gibson, R., Robb, L., Wennhage, H., and Burrows, M. 2002. Ontogenetic changes in depth distribution of juvenile flatfishes in relation to predation risk and temperature on a shallow-water nursery ground. Marine Ecology Progress Series, 229: 233–244.

Hastie, T., and Tibshirani, R. 1986. Generalized additive models. Statistical Science, 1: 14.

Hermann, A. J., Gibson, G. A., Cheng, W., Ortiz, I., Aydin, K., Wang, M., Hollowed, A. B. *et al.* 2019. Projected biophysical conditions of the Bering Sea to 2100 under multiple emission scenarios. ICES Journal of Marine Science, 76: 1937–1937.

Holliday, F. G. T., and Blaxter, J. H. S. 1960. The effects of salinity on the developing eggs and larvae of the herring. Journal of the Marine Biological Association of the United Kingdom, 39: 591–603.

Holsman, K. K., Haynie, A. C., Hollowed, A. B., Reum, J. C. P., Aydin, K., Hermann, A. J., Cheng, W. *et al.* 2020. Ecosystem-based fisheries management forestalls climate-driven collapse. Nature Communications, 11: 4579.

Hunt, G. L., and Stabeno, P. J. 2002. Climate change and the control of energy flow in the southeastern Bering Sea. Progress in Oceanography, 55: 5–22.

IPCC: Summary for Policymakers. 2022. Climate change 2022: impacts, adaptation, and vulnerability. *In* Contribution of Working Group II to the Sixth Assessment Report of the Intergovernmental Panel on Climate Change. Cambridge University Press, Cambridge and New York City, NY.

Ishii, M., Shouji, S., and Matsumoto, T.. 2005. Objective analyses of sea-surface temperature and marine meteorological variables for the 20th century using ICOADS and the Kobe Collection. International Journal of Climatology, 25: 865–879.

Kim, S. S., Lee, C. J., Yoo, H. K., Choi, J., Byun, S. G., Kim, W. J., Lim, H. J. *et al.* 2022. Effect of water temperature on walleye pollock (*Gadus chalcogrammus*) embryos, larvae and juveniles: survival, HSP70 expression, and physiological responses. Aquaculture, 554: 738136.

Kinder, T. H., and Schumacher, J. D. 1981. Hydrographic structure over the continental shelf of the southeastern Bering Sea. Physical Oceanography. https://www.pmel.noaa.gov/pubs/docs/Eastern_Bering_1.4.pdf(last accessed 18 February 2021).

Kjesbu, O. S., and Witthames, P. R. 2007. Evolutionary pressure on reproductive strategies in flatfish and groundfish: relevant concepts and methodological advancements. Journal of Sea Research, 58: 23–34.

Klein, E. S., Smith, S. L., and Kritzer, J. P. 2017. Effects of climate change on four New England groundfish species. Reviews in Fish Biology and Fisheries, 27: 317–338.

Lanksbury, J. A., Duffy-Anderson, J. T., Mier, K. L., Busby, M. S., and Stabeno, P. J. 2007. Distribution and transport patterns of northern rock sole, *Lepidopsetta polyxystra*, larvae in the southeastern Bering Sea. Progress in Oceanography, 72: 39–62.

Laurel, B. J., and Rogers, L. A. 2020. Loss of spawning habitat and prerecruits of Pacific cod during a Gulf of Alaska heatwave. Canadian Journal of Fisheries and Aquatic Sciences, 77: 644–650.

Leathwick, J. R., Elith, J., and Hastie, T. 2006. Comparative performance of generalized additive models and multivariate adaptive regression splines for statistical modelling of species distributions. Ecological Modelling, 199: 188–196.

Lelièvre, S., Vaz, S., Martin, C. S., and Loots, C. 2014. Delineating recurrent fish spawning habitats in the North Sea. Journal of Sea Research, 91: 1–14.

Levin, P. S., Fogarty, M. J., Murawski, S. A., and Fluharty, D. 2009. Integrated ecosystem assessments: developing the scientific basis for ecosystem-based management of the ocean. PLoS Biology, 7: e1000014.

Litzow, M., Bailey, K., Prahl, F., and Heintz, R. 2006. Climate regime shifts and reorganization of fish communities: the essential fatty acid limitation hypothesis. Marine Ecology Progress Series, 315: 1–11.

Logerwell, E. A., Busby, M., Mier, K. L., Tabisola, H., and Duffy-Anderson, J. 2020. The effect of oceanographic variability on the distribution of larval fishes of the northern Bering and Chukchi Seas. Deep Sea Research Part II: Topical Studies in Oceanography, 177: 104784.

Lowerre-Barbieri, S. K., Ganias, K., Saborido-Rey, F., Murua, H., and Hunter, J. R. 2011. Reproductive timing in marine fishes: variability, temporal scales, and methods. Marine and Coastal Fisheries, 3: 71–91.

Luchin, V. A., Menovshchikov, V. A., Lavrentiev, V. M., and Reed, R. K. 1999. Thermohaline structure and water masses in the Bering Sea. *In* Dynamics of the Bering Sea, p. 68. University of Alaska Sea Grant, Fairbanks, AK.

Matarese, A. C., Blood, D. M., Picquelle, S. J., and Benson, J. L. 2003. Atlas of abundance and distribution patterns of ichthyoplankton from the northeast Pacific Ocean and Bering Sea ecosystems based on research conducted by the Alaska Fisheries Science Center (1972–1996). *In* NOAA Prof. Paper NMFS 1. Alaska Fisheries Science Center, Seattle, WA. https://spo.nmfs.noaa.gov/content/atlas-abundance-and-distribution-patterns-ichthyoplankton-northeast-pacific-ocean-and-bering(last accessed 2 June 2021).

McClatchie, S., Thompson, A. R., Alin, S. R., Siedlecki, S., Watson, W., and Bograd, S. J. 2016. The influence of Pacific Equatorial Water on fish diversity in the southern California Current System. Journal of Geophysical Research Oceans, 121: 6121–6136.

McQueen, K., and Marshall, C. T. 2017. Shifts in spawning phenology of cod linked to rising sea temperatures. ICES Journal of Marine Science, 74: 1561–1573.

Mizobata, K., and Saitoh, S. 2004. Variability of Bering Sea eddies and primary productivity along the shelf edge during 1998–2000 using satellite multisensor remote sensing. Journal of Marine Systems, 50: 101–111.

Mizobata, K., Wang, J., and Saitoh, S. 2006. Eddy-induced cross-slope exchange maintaining summer high productivity of the Bering Sea shelf break. Journal of Geophysical Research, 111: 1–14. https://onlinelibrary.wiley.com/doi/abs/10.1029/2005JC003335(last accessed 31 December 2021).

Munk, P. 2016. Larval Fish Ecology—Adaptations and Physical Linkages. Technical University of Denmark, Lyngby. https://orbit.dtu.dk/en/publications/larval-fish-ecology-adaptations-and-physical-linkages(last accessed 4 June 2021).

National Marine Fisheries Service and National Oceanic and Atmospheric Administration. 2021. Fisheries of the Exclusive Economic Zone off Alaska; Bering Sea and Aleutian Islands; Final 2021 and 2022 Harvest Specifications for Groundfish. https://www.federalregister.gov/documents/2021/02/25/2021-03564/fisheries-of-the-exclusive-economic-zone-off-alaska-bering-sea-and-aleutian-islands-final-2021-and(last accessed 24 March 2022).

Neidetcher, S. K., Hurst, T. P., Ciannelli, L., and Logerwell, E. A. 2014. Spawning phenology and geography of Aleutian Islands and eastern Bering Sea Pacific cod (*Gadus macrocephalus*). Deep Sea Research Part II: Topical Studies in Oceanography, 109: 204–214.

NOAA AFSC. 2021. Ichthyoplankton Information System. https://aps-afsc.fisheries.noaa.gov/ichthyo/index.php(last accessed 16 July 2021).

NOAA Fisheries. 2021. Alaska Pollock. https://www.fisheries.noaa.gov/species/alaska-pollock(last accessed 16 July 2021).

NOAA Fisheries. 2022. Stock SMART Data Records. https://apps-st.fisheries.noaa.gov/stocksmart?app=homepage (last accessed 3 August 2021).

O'Leary, C. A., Kotwicki, S., Hoff, G. R., Thorson, J. T., Kulik, V. V., Ianelli, J. N., Lauth, R. R. *et al.* 2021. Estimating spatiotemporal availability of transboundary fishes to fishery-independent surveys. Journal of Applied Ecology, 58: 2146–2157.

Olivar, M. P., and Sabatés, A. 1997. Vertical distribution of fish larvae in the north-west Mediterranean Sea in spring. Marine Biology, 129: 289–300.

Pearcy, W. G., Hosie, M. J., and Richardson, S. L. 1977. Distribution and duration of pelagic life of larvae of Dover sole, *Microstomus pacificus*; Rex sole, *Glyptocephalus zachirus*; and Petrale sole, *Eopsetta jordani*, in waters off Oregon. Fishery Bulletin, 75: 173–183.

Petrik, C. M., Duffy-Anderson, J. T., Castruccio, F., Curchitser, E. N., Danielson, S. L., Hedstrom, K., and Mueter, F. 2016. Modelled connectivity between Walleye pollock (*Gadus chalcogrammus*) spawning and age-0 nursery areas in warm and cold years with implications for juvenile survival. ICES Journal of Marine Science, 73: 1890–1900.

Poloczanska, E. S., Brown, C. J., Sydeman, W. J., Kiessling, W., Schoeman, D. S., Moore, P. J., Brander, K. *et al.* 2013. Global imprint of climate change on marine life. Nature Climate Change, 3: 919–925.

Polyakov, I. V., Alkire, M. B., Bluhm, B. A., Brown, K. A., Carmack, E. C., Chierici, M., Danielson, S. L. *et al.* 2020. Borealization of the Arctic Ocean in response to anomalous advection from sub-Arctic seas. Frontiers in Marine Science, 7: 1–32. https://www.frontiersin.org/articles/10.3389/fmars.2020.00491/full(last accessed 3 August 2021).

Porter, S. 2022. Variation in the distribution of yellowfin sole *Limanda aspera* larvae in warm and cold years in the eastern Bering Sea. Fisheries Oceanography, 31: 108–122.

Porter, S. M., and Ciannelli, L. 2018. Effect of temperature on Flathead sole (*Hippoglossoides elassodon*) spawning in the southeastern Bering Sea during warm and cold years. Journal of Sea Research, 141: 26–36.

R Core Team. 2021. R: A Language and Environment for Statistical Computing. R Foundation for Statistical Computing, Vienna.

Rogers, L. A., and Dougherty, A. B. 2019. Effects of climate and demography on reproductive phenology of a harvested marine fish population. Global Change Biology, 25: 708–720.

Royer, T. C., and Grosch, C. E. 2006. Ocean warming and freshening in the northern Gulf of Alaska. Geophysical Research Letters, 33: 1–6. https://onlinelibrary.wiley.com/doi/abs/10.1029/2006GL026767(last accessed 9 October 2022).

Sambrotto, R. N., Mordy, C., Zeeman, S. I., Stabeno, P. J., and Macklin, S. A. 2008. Physical forcing and nutrient conditions associated with patterns of Chl a and phytoplankton productivity in the southeastern Bering Sea during summer. Deep Sea Research Part II: Topical Studies in Oceanography, 55: 1745–1760.

Sejr, M. K., Stedmon, C. A., Bendtsen, J., Abermann, J., Juul-Pedersen, T., Mortensen, J., and Rysgaard, S. 2017. Evidence of local and regional freshening of northeast Greenland coastal waters. Scientific Reports, 7: 13183.

Servili, A., Canario, A. V. M., Mouchel, O., and Muñoz-Cueto, J. A. 2020. Climate change impacts on fish reproduction are mediated at multiple levels of the brain-pituitary-gonad axis. General and Comparative Endocrinology, 291: 113439.

Sheffield Guy, L., Duffy-Anderson, J., Matarese, A., Mordy, C., Napp, J., and Stabeno, P. 2014. Understanding climate control of fisheries recruitment in the eastern Bering Sea: long-term measurements and process studies. Oceanography, 27: 90–103.

Shima, M., and Bailey, K. M. 1994. Comparative analysis of ichthyoplankton sampling gear for early life stages of walleye pollock (*Theragra chalcogramma*). Fisheries Oceanography, 3: 50–59.

Shotwell, S. K., Pirtle, J. L., Watson, J. T., Deary, A. L., Doyle, M. J., Barbeaux, S. J., Dorn, M. W. *et al.* 2022. Synthesizing integrated ecosystem research to create informed stock-specific indicators for next generation stock assessments. Deep Sea Research Part II: Topical Studies in Oceanography, 198: 105070.

Siddon, E. C., De Forest, L. G., Blood, D. M., Doyle, M. J., and Matarese, A. C. 2019. Early life history ecology for five commercially and ecologically important fish species in the eastern and western Gulf of Alaska. Deep Sea Research Part II: Topical Studies in Oceanography, 165: 7–25.

Siddon, E., Duffy-Anderson, J., and Mueter, F. 2011. Community-level response of fish larvae to environmental variability in the southeastern Bering Sea. Marine Ecology Progress Series, 426: 225–239.

Sims, D. W., Wearmouth, V. J., Genner, M. J., Southward, A. J., and Hawkins, S. J. 2004. Low-temperature-driven early spawning migration of a temperate marine fish. Journal of Animal Ecology, 73: 333–341.

Slesinger, E., Jensen, O. P., and Saba, G. 2021. Spawning phenology of a rapidly shifting marine fish species throughout its range. ICES Journal of Marine Science, 78: 1010–1022.

Smart, T. I., Siddon, E. C., and Duffy-Anderson, J. T. 2013. Vertical distributions of the early life stages of walleye pollock (*Theragra chalcogramma*) in the southeastern Bering Sea. Deep Sea Research Part II: Topical Studies in Oceanography, 94: 201–210.

Spear, A., Napp, J., Ferm, N., and Kimmel, D. 2020. Advection and *in situ* processes as drivers of change for the abundance of large zoo-

plankton taxa in the Chukchi Sea. Deep Sea Research Part II: Topical Studies in Oceanography, 177: 104814.

Spencer, M. L., Vestfals, C. D., Mueter, F. J., and Laurel, B. J. 2020. Ontogenetic changes in the buoyancy and salinity tolerance of eggs and larvae of polar cod (*Boreogadus saida*) and other gadids. Polar Biology, 43: 1141–1158.

Stabeno, P. J., Danielson, S. L., Kachel, D. G., Kachel, N. B., and Mordy, C. W. 2016. Currents and transport on the eastern Bering Sea shelf: an integration of over 20 years of data. Deep Sea Research Part II: Topical Studies in Oceanography, 134: 13–29.

Stabeno, P. J., Duffy-Anderson, J. T., Eisner, L. B., Farley, E. V., Heintz, R. A., and Mordy, C. W. 2017. Return of warm conditions in the southeastern Bering Sea: physics to fluorescence. PLoS One, 12: e0185464.

Swearer, S., Treml, E., and Shima, J. 2019. A review of biophysical models of marine larval dispersal. Oceanography and Marine Biology, 57: 325–356.

TenBrink, T. T. 2022. Delineating yellowfin sole (*Limanda aspera*) reproduction in the northern Bering Sea provides information across the eastern Bering Sea continental shelf. Fisheries Research, 252: 106335.

Vestfals, C. D., Ciannelli, L., Duffy-Anderson, J. T., and Ladd, C. 2014. Effects of seasonal and interannual variability in along-shelf and cross-shelf transport on groundfish recruitment in the eastern Bering Sea. Deep Sea Research Part II: Topical Studies in Oceanography, 109: 190–203.

Wilderbuer, T., Duffy-Anderson, J. T., Stabeno, P., and Hermann, A. 2016. Differential patterns of divergence in ocean drifters: implications for larval flatfish advection and recruitment. Journal of Sea Research, 111: 11–24.

Wilderbuer, T., and Nichol, D.. 2015. BSAI Other Flatfish Assessment. https://apps-afsc.fisheries.noaa.gov/REFM/Docs/2015/BSAIoflat.pdf (last accessed 12 August 2021).

Wood, S. 2017. Generalized Additive Models: An Introduction with R, 2nd edn. Chapman and Hall/CRC, Boca Raton, FL.

Wyllie-Echeverria, T., and Wooster, W. S. 1998. Year-to-year variations in Bering Sea ice cover and some consequences for fish distributions. Fisheries Oceanography, 7: 159–170.

Zhang, C. I., Wilderbuer, T. K., and Walters, G. E. 1998. Biological characteristics and fishery assessment of Alaska plaice, *Pleuronectes quadrituberculatus*, in the eastern Bering Sea. Marine Fisheries Review, 60: 16–27.

Handling editor: Dominique Robert

Received: 17 December 2022; **Revised:** 19 June 2023; **Accepted:** 19 June 2023